Transport-Equilibrium Schemes for Computing Nonclassical Shocks. I. Scalar Conservation Laws

Christophe Chalons *

September 1, 2005

Abstract

This paper presents a very efficient numerical strategy for computing weak solutions of scalar conservation laws which fail to be genuinely nonlinear. We concentrate on the typical situation of either concave-convex or convex-concave flux functions. In such a situation, nonclassical shocks violating the classical Oleinik entropy criterion must be taken into account since they naturally arise as limits of certain diffusive-dispersive regularizations to hyperbolic conservation laws. Such discontinuities play an important part in the resolution of the Riemann problem and their dynamics turns out to be driven by a prescribed *kinetic function* which acts as a selection principle. It aims at imposing the entropy dissipation rate across nonclassical discontinuities, or equivalently their speed of propagation. From a numerical point of view, the serious difficulty consists in enforcing the *kinetic criterion*, that is in controling the numerical entropy dissipation of nonclassical shocks for any given discretization. This is known to be a very challenging issue. By means of an algorithm made of two steps, namely an *Equilibrium step* and a *Transport step*, we show how to force the validity of the kinetic criterion at the discrete level. The resulting scheme provides in addition sharp profiles. Numerical evidences illustrate the validity of our approach.

1 Introduction

We are interested in computing nonclassical weak solutions of an initial-value problem for a scalar conservation law of the form

$$\left\{ \begin{array}{l} \partial_t u + \partial_x f(u) = 0, \;\; u(x,t) \in \mathbb{R}, \;\; (x,t) \in \mathbb{R} \times \mathbb{R}^{+*}, \\ u(x,0) = u_0(x), \end{array} \right. \tag{1}$$

where t is time, x is the one dimensional space variable and $f : \mathbb{R} \to \mathbb{R}$ is a smooth flux-function neither convex nor concave. Generally speaking, it is well-known that due to the nonlinearity of f, solutions of problem (1) may develop discontinuities in finite time and so, are not uniquely determined by initial data u_0. To overcome this difficulty, solutions of (1) may be asked to satisfy, according to a diffusive regularization principle, a full set of entropy inequalities of the form

$$\partial_t U(u) + \partial_x F(u) \leq 0, \quad \forall \; (U,F), \tag{2}$$

where $U : \mathbb{R} \to \mathbb{R}$ and $F : \mathbb{R} \to \mathbb{R}$ are *unspecified* (smooth) functions such that U is convex and $F' = U' f'$. We recall that an equivalent formulation of this selection principle stipulates that any

*Université Paris 7 & Laboratoire JLL, U.M.R. 7598, Boîte courrier 187, 75252 Paris Cedex 05, France. E-mail: chalons@math.jussieu.fr

shock wave solution of (1), separating two constant states u_- and u_+ and propagating with speed σ given by Rankine-Hugoniot conditions, that is

$$u(x,t) = \begin{cases} u_- & \text{if} \quad x < \sigma t, \\ u_+ & \text{if} \quad x > \sigma t, \end{cases} \qquad \text{with} \quad \sigma = \sigma(u_-, u_+) = \frac{f(u_+) - f(u_-)}{u_+ - u_-}, \tag{3}$$

must satisfy Oleinik entropy inequalities

$$\frac{f(v) - f(u_-)}{v - u_-} \geq \frac{f(u_+) - f(u_-)}{u_+ - u_-}, \quad \text{for all } v \text{ between } u_- \text{ et } u_+. \tag{4}$$

In addition, note that selection principles (2) and (4) imply Lax shock inequalities

$$f'(u_-) \geq \sigma \geq f'(u_+). \tag{5}$$

We refer the reader to [16] for additional details. When more general regularizations including diffusive and dispersive terms are considered, solutions of (1) are asked to obey only a single entropy inequality of the form

$$\partial_t U(u) + \partial_x F(u) \leq 0, \tag{6}$$

where $U : \mathbb{R} \to \mathbb{R}$ and $F : \mathbb{R} \to \mathbb{R}$ are now *specified* (smooth) functions, such that U is strictly convex and $F' = U'f'$.

When f is convex or concave, it turns out that all of the entropy conditions (2)-(4)-(5)-(6) are equivalent and actually select a unique *classical* solution of the Riemann problem associated with (1), that is when considering a particular initial data of the form

$$u_0(x) = \begin{cases} u_l & \text{if} \quad x < 0, \\ u_r & \text{if} \quad x > 0, \end{cases} \tag{7}$$

with u_l and u_r two constant states in $\mathbb{R}$. However, the situation becomes more complicated when f fails to be either convex or concave. In such a situation, while conditions (2) and (4) still select equivalently a unique *classical* solution of (1)-(7), it is necessary to supplement the Riemann problem (1)-(7) with an additional selection criterion when the single entropy inequality (6) only is imposed on the solutions. This criterion is called *kinetic relation* from [16]. Basically, there exists many discontinuous solutions (more precisely a one-parameter family of solutions) to the Riemann problem (1)-(6)-(7), all of them except the *classical* one containing a shock wave violating Lax shock inequalities (5). Such discontinuities are often referred as to *undercompressive shocks* or *nonclassical shocks*, and sometimes as to *phase transitions* depending on the context.

In order for the uniqueness of the entropy solution of the Riemann problem (1)-(6)-(7) to be ensured, a *kinetic relation* needs to be added along each nonclassical discontinuity connecting a left-hand state u_- to a right hand state u_+. It aims at imposing the rate of entropy dissipation (6) across admissible nonclassical discontinuities, or equivalently their speed of propagation. Usually, the *kinetic criterion* takes the form

$$u_+ = \varphi^\flat(u_-) \quad \text{or} \quad u_- = \varphi^{-\flat}(u_+) \quad \text{for all nonclassical shock}, \tag{8}$$

where $\varphi^\flat$ is the so-called *kinetic function* and $\varphi^{-\flat}$ its inverse. Again, we refer the reader to [16] for a general theory of nonclassical entropy solutions supplemented with a kinetic relation.

The numerical approximation of nonclassical solutions is known to be very challenging and still constitutes an open problem nowadays. The main difficulty is related to the respect of the kinetic relation at the discrete level. Basically, two strategies exist to approach this problem. The first

one tries to impose the kinetic relation by taking into account the associated small scales, that is the diffusive and dispersive terms that actually generate nonclassical solutions. It amounts to propose a scheme whose equivalent equation best looks like the regularized model with diffusive and dispersive terms. This is usually achieved by means of entropy stable and high-order accurate techniques. In practice, this method provides satisfactory results for shocks with *small strength*, but shocks with *large strength* are not properly captured due to the great sensitivity of nonclassical shocks with respect to numerical diffusion and small scales in general. For more details, we refer for instance to [11], [12], [17], [7], [8] or [3] and the references therein. The second strategy, known under the name of "sharp interface approach", deals directly with the kinetic function $\varphi^\flat$ to tackle the dynamics of nonclassical solutions. In this context, the front tracking scheme and Glimm's random choice scheme are free of artificial numerical diffusion and then give *sharp* nonclassical shocks satisfying the prescribed kinetic relation. But these methods actually rely on the knowledge of the underlying nonclassical Riemann solution, which prevents any complex application. See for instance [15], [9], [2], [13], [14].

In this paper, we present a new scheme based on a "sharp interface approach" for capturing discontinuities whose dynamics is driven by a prescribed kinetic function. By construction, our scheme gives sharp isolated nonclassical shocks, but contrarily to Glimm's random choice scheme for instance it does not explicitly use the solution of the corresponding nonclassical Riemann solver. The resulting algorithm is essentially conservative and provides numerical results in full agreement with exact ones, whatever the strength of the shocks are. In some sense, our algorithm keeps advantages of Glimm's random choice scheme (sharp interfaces propagating at the right speed) and leaves its main drawbacks (the need of the nonclassical Riemann solutions).

2 Nonclassical Riemann solvers for concave-convex and convex-concave flux functions

In this section, we follow [16] and review the theory of nonclassical Riemann solutions to (1)-(6)-(7)-(8) in the non restrictive situation when the flux function f is either concave-convex, in the sense that

$$\begin{array}{c} uf''(u) > 0 \quad \text{when} \quad u \neq 0, \quad f'''(0) \neq 0, \\ \text{and} \quad \lim_{|u|\to+\infty} f'(u) = +\infty, \end{array} \tag{9}$$

or convex-concave in the sense that

$$\begin{array}{c} uf''(u) < 0 \quad \text{when} \quad u \neq 0, \quad f'''(0) \neq 0, \\ \text{and} \quad \lim_{|u|\to+\infty} f'(u) = -\infty. \end{array} \tag{10}$$

Such flux functions have an unique inflection point at $u = 0$. Typically, we will consider the two cases $f(u) = u^3$ and $f(u) = -u^3$ in Section 4 devoted to numerical experiments.

Following [16], we first define function $\varphi^\natural : \mathbb{R} \to \mathbb{R}$ related to the graph of function f in the (u, f)-plane as follows : for any $u \neq 0$, $\varphi^\natural(u) \neq u$ is the unique value such that the line passing through the points $(u, f(u))$ and $(\varphi^\natural(u), f(\varphi^\natural(u)))$ is tangent to the graph of function f at point $(\varphi^\natural(u), f(\varphi^\natural(u)))$:

$$f'(\varphi^\natural(u)) = \frac{f(u) - f(\varphi^\natural(u))}{u - \varphi^\natural(u)}.$$

Setting $\varphi^\natural(0) = 0$, function $\varphi^\natural : \mathbb{R} \to \mathbb{R}$ is seen to be smooth, monotone decreasing and onto thanks to (9) or (10). We denote $\varphi^{-\natural} : \mathbb{R} \to \mathbb{R}$ its inverse function. It turns out that functions $\varphi^\natural$ and $\varphi^{-\natural}$ play an important role when addressing the single entropy inequality (6) for discontinuous solutions.

More precisely, considering a shock wave solution of (1) of the form (3), entropy inequality (6) holds in the integrale sense if and only if the entropy dissipation

$$E(u_-,u_+)=-\sigma(u_-,u_+)(U(u_+)-U(u_-))+(F(u_+)-F(u_-))$$

is such that $E(u_-,u_+)\leq 0$. Well, it is proved in [16] that function $u_+\to E(u_-,u_+)$ achieves a maximum negative (respectively positive) value at $u_+=\varphi^\natural(u_-)$ when f is concave-convex (respectively convex-concave), while vanishing exactly twice at u_- and let us say $\varphi_0^\flat(u_-)\in[\varphi^{-\natural}(u_-),\varphi^\natural(u_-)]$. Moreover, assuming that $u_->0$ we have $E(u_-,u_+)<0$ if $u_+\in(\varphi_0^\flat(u_-),\varphi^\natural(u_-))$ (respectively $u_+\in(\varphi^{-\natural}(u_-),\varphi_0^\flat(u_-))$ when f is concave-convex (respectively convex-concave). This will motivate assumptions (11) and (12) made on kinetic function $\varphi^\flat$ applied to select nonclassical shock waves.

From $\varphi^\flat$, we also define the function $\varphi^\sharp:\mathbb{R}\to\mathbb{R}$ such that the line passing through the points $(u,f(u))$ and $(\varphi^\flat(u),f(\varphi^\flat(u)))$ with $u\neq 0$ also cut the graph of function f at point $(\varphi^\sharp(u),f(\varphi^\sharp(u)))$ with $\varphi^\sharp(u)\neq u$ and $\varphi^\sharp(u)\neq\varphi^\flat(u)$:

$$\frac{f(u)-f(\varphi^\flat(u))}{u-\varphi^\flat(u)}=\frac{f(u)-f(\varphi^\sharp(u))}{u-\varphi^\sharp(u)}.$$

More generally, we define $\rho(u,v)\in\mathbb{R}$ if $v\neq u$ and $v\neq\varphi^\natural(u)$ by

$$\frac{f(\rho(u,v))-f(u)}{\rho(u,v)-u}=\frac{f(v)-f(u)}{v-u}$$

with $\rho(u,v)\neq u$ and $\rho(u,v)\neq v$, and extend function ρ by continuity otherwise. Of course, we note that $\varphi^\sharp(u)=\rho(u,\varphi^\flat(u))$. We are now in position to give the nonclassical Riemann solver associated with (1)-(6)-(7)-(8), see [16].

The case of a concave-convex flux function :

Let us assume that f obeys (9) and let $\varphi^\flat:\mathbb{R}\to\mathbb{R}$ be a kinetic function, that is (by definition) a monotone decreasing and Lipschitz continuous mapping such that

$$\left\{\begin{array}{ll}\varphi_0^\flat(u)<\varphi^\flat(u)\leq\varphi^\natural(u) & \text{if}\quad u>0,\\ \varphi^\natural(u)\leq\varphi^\flat(u)<\varphi_0^\flat(u) & \text{if}\quad u<0.\end{array}\right. \tag{11}$$

Then, the nonclassical Riemann solver associated with (1)-(6)-(7)-(8) is given as follows.
When $u_l>0$:

(1) If $u_r\geq u_l$, the solution is a rarefaction wave connecting u_l to u_r.

(2) If $u_r\in[\varphi^\sharp(u_l),u_l)$, the solution is a classical shock wave connecting u_l to u_r.

(3) If $u_r\in(\varphi^\flat(u_l),\varphi^\sharp(u_l))$, the solution contains a nonclassical shock connecting u_l to $\varphi^\flat(u_l)$, followed by a classical shock connecting $\varphi^\flat(u_l)$ to u_r.

(4) If $u_r\leq\varphi^\flat(u_l)$, the solution contains a nonclassical shock connecting u_l to $\varphi^\flat(u_l)$, followed by a rarefaction connecting $\varphi^\flat(u_l)$ to u_r.

When $u_l\leq 0$:

(1) If $u_r\leq u_l$, the solution is a rarefaction wave connecting u_l to u_r.

(2) If $u_r\in[u_l,\varphi^\sharp(u_l))$, the solution is a classical shock wave connecting u_l to u_r.

(3) If $u_r\in(\varphi^\sharp(u_l),\varphi^\flat(u_l))$, the solution contains a nonclassical shock connecting u_l to $\varphi^\flat(u_l)$, followed by a classical shock connecting $\varphi^\flat(u_l)$ to u_r.

(4) If $u_r\geq\varphi^\flat(u_l)$, the solution contains a nonclassical shock connecting u_l to $\varphi^\flat(u_l)$, followed by a rarefaction connecting $\varphi^\flat(u_l)$ to u_r.

The case of a convex-concave flux function :

Let us assume that f obeys (10) and let $\varphi^\flat : \mathbb{R} \to \mathbb{R}$ be a kinetic function, that is (again by definition) a monotone decreasing and Lipschitz continuous mapping such that

$$\left\{ \begin{array}{ll} \varphi_0^\flat(u) < \varphi^\flat(u) \leq \varphi^{-\natural}(u) & \text{if} \quad u < 0, \\ \varphi^{-\natural}(u) \leq \varphi^\flat(u) < \varphi_0^\flat(u) & \text{if} \quad u > 0. \end{array} \right. \tag{12}$$

Then, the nonclassical Riemann solver associated with (1)-(6)-(7)-(8) is given as follows.
When $u_l > 0$:

(1) If $u_r \geq u_l$, the solution is a classical shock connecting u_l to u_r.

(2) If $u_r \in [0, u_l)$, the solution is a rarefaction wave connecting u_l to u_r.

(3) If $u_r \in (\varphi^\flat(u_l), 0)$, the solution contains a rarefaction wave connecting u_l to $\varphi^{-\flat}(u_r)$, followed by a nonclassical shock connecting $\varphi^{-\flat}(u_r)$ to u_r.

(4) If $u_r \leq \varphi^\flat(u_l)$, the solution contains :

(i) a classical shock connecting u_l to $\varphi^{-\flat}(u_r)$, followed by a nonclassical shock connecting $\varphi^{-\flat}(u_r)$ to u_r, if $u_l > \rho(\varphi^{-\flat}(u_r), u_r)$.

(ii) a classical shock connecting u_l to u_r, if $u_l \leq \rho(\varphi^{-\flat}(u_r), u_r)$.

When $u_l \leq 0$:

(1) If $u_r \leq u_l$, the solution is a classical shock connecting u_l to u_r.

(2) If $u_r \in (u_l, 0]$, the solution is a rarefaction wave connecting u_l to u_r.

(3) If $u_r \in (0, \varphi^\flat(u_l))$, the solution contains a rarefaction wave connecting u_l to $\varphi^{-\flat}(u_r)$, followed by a non classical shock connecting $\varphi^{-\flat}(u_r)$ to u_r.

(4) If $u_r \geq \varphi^\flat(u_l)$, the solution contains :

(i) a classical shock connecting u_l to $\varphi^{-\flat}(u_r)$, followed by a nonclassical shock connecting $\varphi^{-\flat}(u_r)$ to u_r, if $u_l < \rho(\varphi^{-\flat}(u_r), u_r)$.

(ii) a classical shock connecting u_l to u_r, if $u_l \geq \rho(\varphi^{-\flat}(u_r), u_r)$.

3 Numerical approximation

In this section, we present a suitable algorithm for approximating the nonclassical Riemann solutions of (1)-(6)-(7)-(8). Let us first introduce some notations. We assume as given a constant time step Δt and a constant space step Δx, and we denote $x_{j+1/2} = j\Delta x$ for $j \in \mathbb{Z}$ the interfaces and $t^n = n\Delta t$ for $n \in \mathbb{N}$ the intermediate times. Then, we seek at each time t^n a constant approximation u_j^n of solution $x \to u(x, t^n)$ on each interval $C_j = [x_{j-1/2}; x_{j+1/2})$ and for all $j \in \mathbb{Z}$.

From previous sections, it is clear that most of the theoretical as well as numerical difficulties are a direct consequence of existence of areas having different convexity properties on the graph of function f. That is the reason why we will only focus ourselves, in a first approach at least (see indeed Section 5 for the general case), on the most difficult solutions to capture numerically, that is those joigning areas having a different convexity. When f obeys either (9) or (10), it is a matter of solutions separating two states u_- and u_+ such that $u_- u_+ < 0$. Concerning the solutions remaining always either in $\mathbb{R}^-$ or $\mathbb{R}^+$, we choose from now on a numerical flux function g consistent with the flux fonction f and consider the following 3-point explicit conservative scheme to numerically solve (1):

$$u_j^{n+1} = u_j^n - \lambda(g_{j+1/2} - g_{j-1/2}), \quad j \in \mathbb{Z}, \tag{13}$$

with $\lambda = \dfrac{\Delta t}{\Delta x}$ and $g_{j+1/2} = g(u_j^n, u_{j+1}^n)$ for all $j \in \mathbb{Z}$. The question is now to understand how to modify such a conservative scheme in order to properly capture all the solutions of the Riemann problem (1)-(6)-(7)-(8), that is including those associated with the case $u_l u_r < 0$ in (7).

With this in mind, let us introduce two subsets $\mathcal{C}$ and $\mathcal{N}$ made of all the pairs $(u_l, u_r) \in \mathbb{R}^2$ with $u_l u_r < 0$ and such that the Riemann solution of (1)-(6)-(7)-(8) is respectively classical and nonclassical. In view of previous section, we thus have :

$$\mathcal{C} = \tag{14}$$

$$\left| \begin{array}{l} \{(u_l, u_r),\ u_l u_r < 0 \ /\ u_l u_r \geq u_l \varphi^\sharp(u_l)\} \text{ if f obeys (9)}, \\ \{(u_l, u_r),\ u_l u_r < 0 \ /\ u_l u_r \leq u_l \varphi^\flat(u_l) \text{ and } u_l^2 \leq u_l \rho(\varphi^{-\flat}(u_r), u_r)\} \text{ if f obeys (10)}, \end{array} \right.$$

and

$$\mathcal{N} = \tag{15}$$

$$\left| \begin{array}{l} \{(u_l, u_r),\ u_l u_r < 0 \ /\ u_l u_r < u_l \varphi^\sharp(u_l)\} \text{ if f obeys (9)}, \\ \{(u_l, u_r),\ u_l u_r < 0 \ /\ \{u_l u_r > u_l \varphi^\flat(u_l)\} \text{ or } \{u_l u_r \leq u_l \varphi^\flat(u_l) \text{ and } u_l^2 > u_l \rho(\varphi^{-\flat}(u_r), u_r)\} \text{ if f obeys (10)}. \end{array} \right.$$

Remark that $\mathcal{C} = \emptyset$ if f obeys (9) and $u_l \varphi^\sharp(u_l) \geq 0$. Moreover, the Riemann solution associated with a pair (u_l, u_r) in $\mathcal{C}$ (when not empty) is always a classical shock connecting u_l to u_r while if (u_l, u_r) belongs to $\mathcal{N}$, the Riemann solution is nonclassical and composite (made of two waves) except if $u_r = \varphi^\flat(u_l)$. In the latter case, the solution simply consists in a nonclassical shock from u_l to u_r since the kinetic criterion is respected.

Actually, the basic motivation in the construction of our algorithm is double. First of all, we observe that when Riemann initial data (7) is such that both $u_l u_r < 0$ and the corresponding solution is simply a shock wave (either classical or nonclassical) from u_l to u_r, it is a pity that spurious values distinct from u_l and u_r are created by conservative scheme (13). Indeed, considering the following natural discretization of (7)

$$u_j^0 = \left\{ \begin{array}{ll} u_l & \text{if} \quad j \leq 0, \\ u_r & \text{if} \quad j \geq 1, \end{array} \right. \tag{16}$$

we get

$$u_j^1 = \left\{ \begin{array}{ll} u_l - \lambda(g(u_l, u_l) - g(u_l, u_l)) = u_l & \text{if} \quad j \leq -1, \\ u_l - \lambda(g(u_l, u_r) - g(u_l, u_l)) & \text{if} \quad j = 0, \\ u_r - \lambda(g(u_r, u_r) - g(u_l, u_r)) & \text{if} \quad j = 1, \\ u_r - \lambda(g(u_r, u_r) - g(u_r, u_r)) = u_r & \text{if} \quad j \geq 2. \end{array} \right.$$

with, generally speaking, $u_0^1 \notin \{u_l, u_r\}$ and $u_1^1 \notin \{u_l, u_r\}$. Instead, we would prefer to keep a sharp interface between u_l and u_r, propagating at speed σ given by Rankine-Hugoniot conditions, namely $\sigma = \sigma(u_l, u_r)$ with

$$\sigma(u, v) = \frac{f(u) - f(v)}{u - v},\ \forall\ u \neq v. \tag{17}$$

To achieve this goal, we suggest to apply the following nonconservative formula :

$$u_j^{n+1} = u_j^n - \lambda(g_{j+1/2}^L - g_{j-1/2}^R), \quad j \in \mathbb{Z}, \tag{18}$$

where the numerical fluxes $g_{j+1/2}^L = g_{j+1/2}^L(u_j^n, u_{j+1}^n)$ and $g_{j+1/2}^R = g_{j+1/2}^R(u_j^n, u_{j+1}^n)$ have to be suitably defined. First of all, it is natural to set

$$g_{j+1/2}^L(u, u) = g_{j+1/2}^R(u, u) = g(u, u), \quad j \in \mathbb{Z},$$

for all u. Then, if u_l and u_r such that $u_l u_r < 0$ are connected by a classical shock (that is $(u_l, u_r) \in \mathcal{C}$), setting

$$g_{j+1/2}^L(u_l, u_r) = g(u_l, u_l) \quad \text{and} \quad g_{j+1/2}^R(u_l, u_r) = g(u_r, u_r), \quad j \in \mathbb{Z}, \tag{19}$$

is sufficient to avoid spurious intermediate values since we get

$$\left\{\begin{array}{l} u_0^1 = u_l - \lambda(g^L_{1/2}(u_l,u_r) - g^R_{-1/2}(u_l,u_l)) = u_l - \lambda(g(u_l,u_l) - g(u_l,u_l)) = u_l, \\ u_1^1 = u_r - \lambda(g^L_{3/2}(u_r,u_r) - g^L_{1/2}(u_l,u_r)) = u_r - \lambda(g(u_r,u_r) - g(u_r,u_r)) = u_r. \end{array}\right.$$

In the same way, if u_l and $u_r = \varphi^\flat(u_l)$ are connected by a nonclassical shock (in particular $(u_l,u_r) \in \mathcal{N}$), setting

$$g^L_{j+1/2}(u_l,u_r) = g(u_l,\varphi^{-\flat}(u_r)) \quad \text{and} \quad g^R_{j+1/2}(u_l,u_r) = g(\varphi^\flat(u_l),u_r), \quad j \in \mathbb{Z}, \tag{20}$$

is fitting since

$$\left\{\begin{array}{l} u_0^1 = u_l - \lambda(g^L_{1/2}(u_l,u_r) - g^R_{-1/2}(u_l,u_l)) = u_l - \lambda(g(u_l,u_l) - g(u_l,u_l)) = u_l, \\ u_1^1 = u_r - \lambda(g^L_{3/2}(u_r,u_r) - g^L_{1/2}(u_l,u_r)) = u_r - \lambda(g(u_r,u_r) - g(u_r,u_r)) = u_r. \end{array}\right.$$

Thanks to the new update formula (18), we are thus able to remove nondesired values. Nevertheless, it is clear at this stage that initial discretization (16) is made stationary by this new update formula, when it should be moving at speed $\sigma(u_l,u_r)$ given by (17). A transport step must thus be included in our algorithm. In the whole description of the numerical strategy below, we will use a sampling procedure in order to avoid emergence of new spurious values.

The second motivation in the installation of our algorithm concerns the situations $(u_l,u_r) \in \mathcal{N}$ but $u_r \neq \varphi^\flat(u_l)$, when a nonclassical shock which is not initially present in initial data (7) is generated by the nonclassical Riemann solver. We would like to force the numerical scheme to create such a nonclassical discontinuity. That is the reason why we propose to use (20) as soon as $(u_l,u_r) \in \mathcal{N}$, *i.e.* even if $u_r \neq \varphi^\flat(u_l)$.

We now describe our algorithm in details. As motivated above, the method is made of two steps : an *Equilibrium step* and a *Transport step*. In the equilibrium step, we propose to modify any given consistent and conservative scheme of the form (13) in order to put at stationary equilibrium certain admissible discontinuities. Then, the transport step aims at propagating these discontinuities. It is worth noticing that the resulting scheme really uses few things coming from the nonclassical Riemann solver, namely only informations concerning the appearance of nonclassical shocks via sets $\mathcal{C}$ and $\mathcal{N}$. But in no way the Riemann solution itself. That represents a considerable profit compared to Glimm's random choice scheme for instance.

First step $(t^n \to t^{n+1-})$ This first step aims at making stationary some of admissible discontinuities of problem (1)-(6)-(7)-(8). We thus consider the nonconservative version (18) of (13) where the numerical fluxes $g^L_{j+1/2}$ and $g^R_{j+1/2}$ are defined as follows for all $j \in \mathbb{Z}$:

$$g^L_{j+1/2} = g^L_{j+1/2}(u_j^n,u_{j+1}^n) = \left\{\begin{array}{ccc} g(u_j^n,u_j^n) & \text{if} & (u_j^n,u_{j+1}^n) \in \mathcal{C}, \\ g(u_j^n,\varphi^{-\flat}(u_{j+1}^n)) & \text{if} & (u_j^n,u_{j+1}^n) \in \mathcal{N}, \\ g_{j+1/2} = g(u_j^n,u_{j+1}^n) & \text{otherwise,} & \end{array}\right. \tag{21}$$

and

$$g^R_{j+1/2} = g^R_{j+1/2}(u_j^n,u_{j+1}^n) = \left\{\begin{array}{ccc} g(u_{j+1}^n,u_{j+1}^n) & \text{if} & (u_j^n,u_{j+1}^n) \in \mathcal{C}, \\ g(\varphi^\flat(u_j^n),u_{j+1}^n) & \text{if} & (u_j^n,u_{j+1}^n) \in \mathcal{N}, \\ g_{j+1/2} = g(u_j^n,u_{j+1}^n) & \text{otherwise.} & \end{array}\right. \tag{22}$$

Second step ($t^{n+1-} \to t^{n+1}$) This step is concerned with the transport of the solution obtained at time t^{n+1-}, and more precisely with the dynamics of discontinuities left stationary during the first step. We first recall that the speed of propagation $\sigma(u_-, u_+)$ of a discontinuity between u_- and u_+ is given by Rankine-Hugoniot conditions (17). We then define at each interface $x_{j+1/2}$ a speed of propagation $\sigma_{j+1/2}$ by naturally setting :

$$\sigma_{j+1/2} = \begin{cases} \sigma(u_j^{n+1-}, u_{j+1}^{n+1-}) & \text{if} \quad (u_j^n, u_{j+1}^n) \in \mathcal{C} \cup \mathcal{N}, \\ 0 & \text{otherwise,} \end{cases} \tag{23}$$

and solve locally (at each discontinuity $x_{j+1/2}$) a transport equation with speed $\sigma_{j+1/2}$. In order to get a new approximation u_j^{n+1} at time $t^{n+1} = t^n + \Delta t$, we then propose to pick randomly on interval $[x_{j-1/2}, x_{j+1/2})$ a value in the juxtaposition of these Riemann solutions at time Δt chosen sufficiently small to avoid wave interactions. More precisely, given a well distributed random sequence (a_n) within interval $(0, 1)$, it amounts to set :

$$u_j^{n+1} = \begin{cases} u_{j-1}^{n+1-} & \text{if} \quad a_{n+1} \in (0, \lambda\sigma_{j-1/2}^+), \\ u_j^{n+1-} & \text{if} \quad a_{n+1} \in [\lambda\sigma_{j-1/2}^+, 1 + \lambda\sigma_{j+1/2}^-), \\ u_{j+1}^{n+1-} & \text{if} \quad a_{n+1} \in [1 + \lambda\sigma_{j+1/2}^-, 1), \end{cases} \tag{24}$$

with $\sigma_{j+1/2}^+ = \max(\sigma_{j+1/2}, 0)$ and $\sigma_{j+1/2}^- = \min(\sigma_{j+1/2}, 0)$ for all $j \in \mathbb{Z}$. This concludes the description of our numerical strategy.

4 Numerical experiments

In this section, we propose some numerical evidences in order to illustrate the relevance of the transport-equilibrium scheme we have proposed. To that purpose, we consider without loss of generality the cubic flux functions $f(u) = \varepsilon u^3$ with $\varepsilon = \pm 1$ which are to some extent the simplest examples of concave-convex ($\varepsilon = 1$) and convex-concave ($\varepsilon = -1$) functions. System (1) now reads

$$\begin{cases} \partial_t u + \partial_x \varepsilon u^3 = 0, \;\; u(x,t) \in \mathbb{R}, \;\; (x,t) \in \mathbb{R} \times \mathbb{R}^{+*}, \\ u(x,0) = u_0(x). \end{cases} \tag{25}$$

Our objective is to compute weak solutions of (25) satisfying entropy inequality

$$\partial_t u^2 + \frac{3}{2}\varepsilon\, \partial_x u^4 \leq 0, \tag{26}$$

that is $U(u) = u^2$ and $F(u) = \dfrac{3}{2}\varepsilon u^4$ in (6). Easy calculations lead to

$$\varphi^\natural(u) = -\frac{u}{2} \quad \text{and} \quad \varphi_0^\flat(u) = -u,$$

so that (11) when $\varepsilon = 1$ and (12) when $\varepsilon = -1$ permit us (again without restriction) to consider a kinetic function of the form

$$\varphi^\flat(u) = -\beta^\varepsilon\, u, \quad \varphi^{-\flat}(u) = -\beta^{-\varepsilon}\, u, \tag{27}$$

with $\beta \in [1/2, 1)$. More precisely, we take $\beta = 3/4$. It is also easy to obtain

$$\rho(u, v) = -u - v \quad \text{and} \quad \varphi^\sharp(u) = (\beta^\varepsilon - 1)u.$$

Concerning the basic numerical flux g, we consider a Roe scheme, that is

$$g(u,v) = \begin{cases} f(u) & \text{if} \quad a(u,v) \geq 0, \\ f(v) & \text{if} \quad a(u,v) < 0, \end{cases} \qquad \text{with} \qquad a(u,v) = \begin{cases} \frac{f(u)-f(v)}{u-v} & \text{if} \quad u \neq v, \\ 0 & \text{if} \quad u = v, \end{cases} \tag{28}$$

and following a proposal by Collela [10], we use van der Corput random sequence (a_n) defined by

$$a_n = \sum_{k=0}^{m} i_k 2^{-(k+1)},$$

where $n = \sum_{k=0}^{m} i_k 2^k$, $i_k = 0, 1$, denotes the binary expansion of the integers $n = 1, 2, ...$

Let us now validate our numerical strategy by considering the typical behaviors of the Riemann solutions given in Section 2. We thus consider initial data of the form (7). When $f(u) = u^3$ (*i.e.* $\varepsilon = 1$), we take $u_l = 4$ and u_r respectively such that

Test $\mathbf{A}^1$: $u_r = 5$, *i.e.* $u_r > u_l$,

Test $\mathbf{B}^1$: $u_r = -0.5$, *i.e.* $u_r \in (\varphi^\sharp(u_l), u_l)$,

Test $\mathbf{C}^1$: $u_r = -2$, *i.e.* $u_r \in (\varphi^\flat(u_l), \varphi^\sharp(u_l))$,

Test $\mathbf{D}^1$: $u_r = -5$, *i.e.* $u_r < \varphi^\flat(u_l)$.

Numerical solutions are plotted on Figures 1 and 2. When $f(u) = -u^3$ (*i.e.* $\varepsilon = -1$), we take $u_l = 3$ and u_r respectively such that

Test $\mathbf{A}^{-1}$: $u_r = 4$, *i.e.* $u_r > u_l$,

Test $\mathbf{B}^{-1}$: $u_r = 2$, *i.e.* $u_r \in (0, u_l)$,

Test $\mathbf{C}^{-1}$: $u_r = -2$, *i.e.* $u_r \in (\varphi^\flat(u_l), 0)$,

Test $\mathbf{D}^{-1}$: $u_r = -8$, *i.e.* $u_r < \varphi^\flat(u_l)$ and $u_l > \rho(\varphi^{-\flat}(u_r), u_r)$,

Test $\mathbf{E}^{-1}$: $u_r = -16$, *i.e.* $u_r < \varphi^\flat(u_l)$ and $u_l < \rho(\varphi^{-\flat}(u_r), u_r)$.

Numerical solutions are plotted on Figures 3, 4 and 5. The mesh contains 100 points per unit interval.

In all these situations, we observe that numerical solutions fully agree with exact ones. In simulations A^1 (Figure 1 - Left) and B^{-1} (Figure 3 - Right), the solution is a single rarefaction wave remaining in a region of convexity and concavity of f, so that our algorithm exactly coincides with the Roe scheme. It is the same for simulation A^{-1} (Figure 3 - Left) for which the solution is a classical shock lying in a region of concavity of f. In simulations B^1 (Figure 1 - Right) and E^{-1} (Figure 5), the solution consists in a single classical shock wave, but connecting a convex region and a concave region of f, so that our two steps algorithm actually operates and provides by construction a sharp discontinuity. Basically, our algorithm exactly coincides with Glimm's random choice scheme for these test cases. In the last four Riemann problems (Figure 2 - Left and Right and Figure 4 - Left and Right), the solutions contain classical as well as nonclassical waves. Here again, we observe that the left and right states of the nonclassical waves are exactly captured while there are not any points in the profiles. Note that the kinetic criterion is respected perfectly.

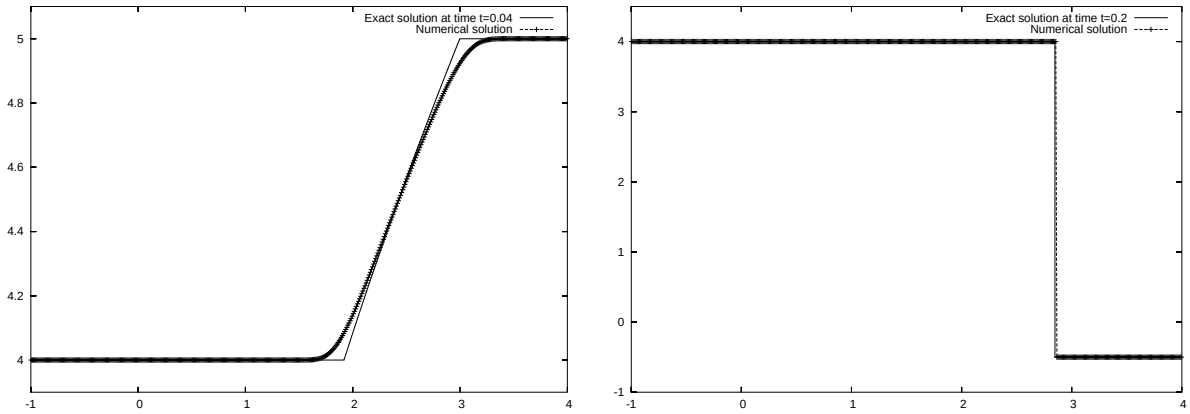

Figure 1: Classical solutions : test A^1 (Left) and B^1 (Right)

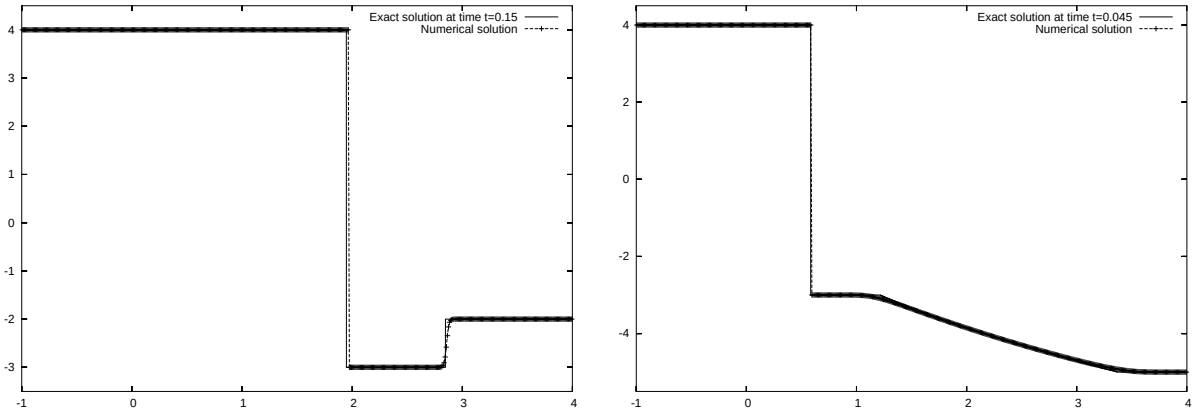

Figure 2: Nonclassical solutions : test C^1 (Left) and D^1 (Right)

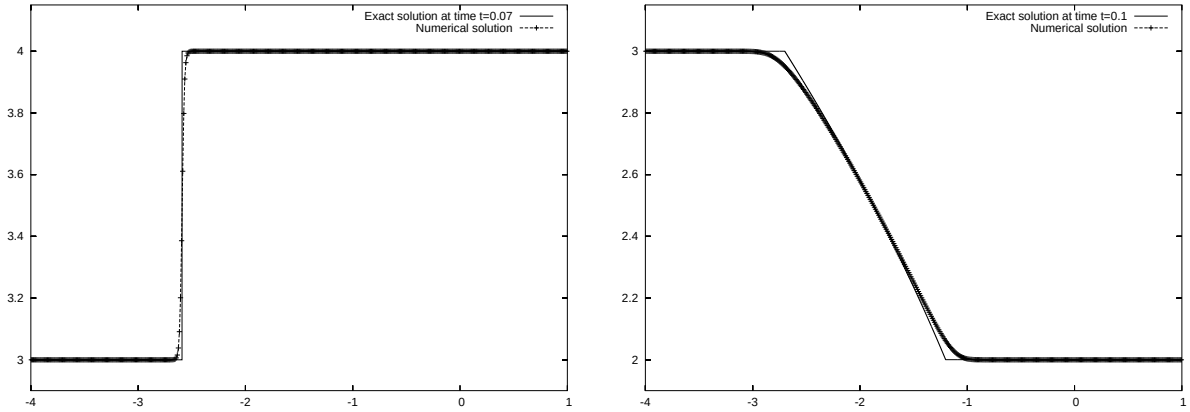

Figure 3: Classical solutions : test A^{-1} (Left) and B^{-1} (Right)

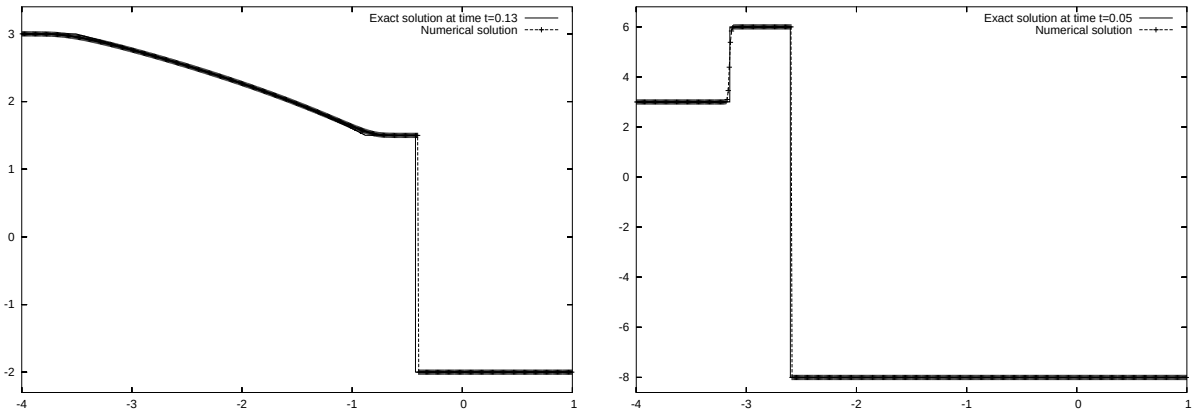

Figure 4: Nonclassical solutions : test C^{-1} (Left) and D^{-1} (Right)

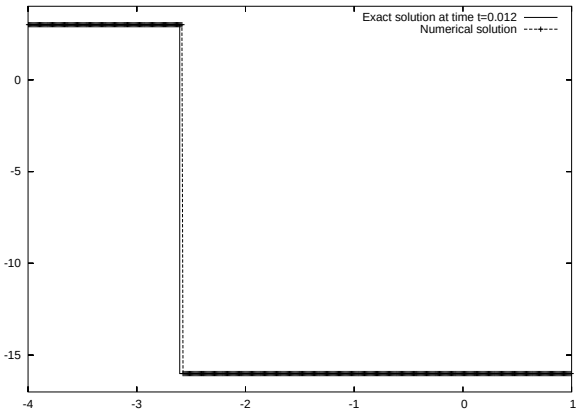

Figure 5: Classical solution : test E^{-1}

5 Towards sharp classical and nonclassical shocks

We conclude this section by paying a particular attention to the test cases C^1, A^{-1} and D^{-1}. Figure 2 - Left, Figure 3 - Left and Figure 4 - Right show that the solution is composed of classical and/or nonclassical shocks. From a numerical point of view, we note that the nonclassical waves are sharp, while the classical ones contain numerical diffusion induced by the Roe scheme. To cure this problem, we are thus tempted to slightly modify the definitions of the numerical fluxes $g^L_{j+1/2}$ and $g^R_{j+1/2}$ in (21)-(22) so that all the shocks (classical as well as nonclassical) are kept at equilibrium during the first step. This is done by including classical shocks remaining in a same region of convexity of f in the definition of $\mathcal{C}$ in (14). We get

$$\mathcal{C} = \tag{29}$$

$$\left| \begin{array}{l} \{(u_l,u_r) \ / \ u_l\varphi^\sharp(u_l) \le u_l u_r < u_l^2\} \text{ if f obeys (9),} \\ \{(u_l,u_r) \ / \ \{u_l^2 < u_l u_r\} \text{ or } \{u_l u_r \le u_l\varphi^\flat(u_l) \text{ and } u_l^2 \le u_l\rho(\varphi^{-\flat}(u_r),u_r)\}\} \text{ if f obeys (10).} \end{array} \right.$$

The numerical speed of propagation $\sigma_{j+1/2}$ is still defined by (23) but of course with the new definition of $\mathcal{C}$ above. Note that such an approach is more detailed and also applied to systems of conservation laws in a follow-up paper [6]. Figures 6 and 7 represent the numerical solutions obtained with this *modified* algorithm. As expected, both type of shocks are sharp.

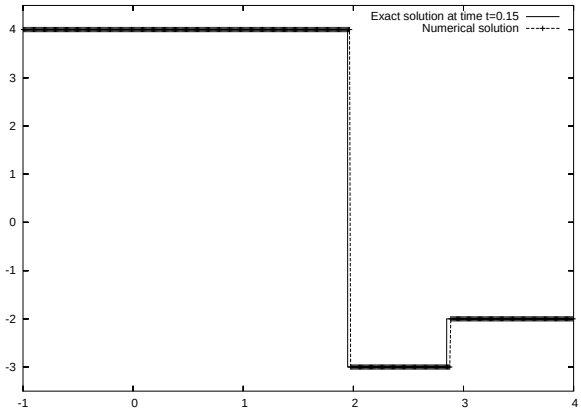

Figure 6: Nonclassical solution with the *modified* algorithm : test C^1

6 Conservation errors

The transport-equilibrium algorithm we have proposed is clearly nonconservative since two numerical fluxes g^L and g^R are used in the first step, and that the transport step is based on a random sampling. In this section, we propose to measure the conservation error on numerical solution u_λ defined as

$$u_\lambda(x,t) = u_j^n \quad \text{if} \quad (x,t) \in [x_{j-1/2}; x_{j+1/2}) \times [t^n; t^{n+1}).$$

Let us first recall that exact solution u evolves according to

$$\partial_t u + \partial_x f(u) = 0,$$

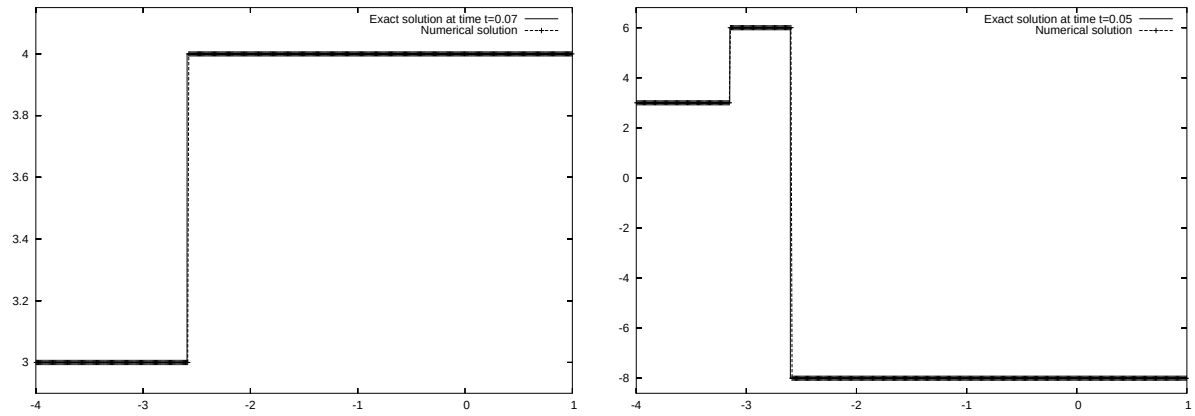

Figure 7: Nonclassical solution with the *modified* algorithm : test A^{-1} (Left) and D^{-1} (Right)

so that by integrating this equation between times $t = 0$ and $t = T > 0$ on computational domain $[x_0, x_1]$ of $\mathbb{R}_x$, we easily get

$$\int_{x_0}^{x_1} u(x,T)dx - \int_{x_0}^{x_1} u_0(x)dx + \int_0^T f(u(x_1,t))dt - \int_0^T f(u(x_0,t))dt = 0. \tag{30}$$

Our objective is to get information about the validity of this equality at the discrete level. We propose for that to compare with 0 the fonction $E : T \in \mathbb{R}^+ \to E(T) \in \mathbb{R}$ with $E(T)$ defined by relation

$$\int_{x_0}^{x_1} u_\lambda(x,T)dx \times E(T) \;=\; \int_{x_0}^{x_1} u_\lambda(x,T)dx - \int_{x_0}^{x_1} u_\lambda(x,0)dx + \int_0^T f(u_\lambda(x_1,t))dt - \int_0^T f(u_\lambda(x_0,t))dt. \tag{31}$$

Recall that u_λ is piecewise constant so that the evaluation of $E(T)$ does not raise any difficulty. In addition, it is worth noticing that if $f(u_\lambda(x_0,t))$ and $f(u_\lambda(x_1,t))$ coincide for all $t \in [0,T]$ with the corresponding exact values $f(u(x_0,t))$ and $f(u(x_1,t))$ (this is in particular the case when the dynamics of the numerical solution did not reach yet the boundaries x_0 and x_1 of the computational domain) and that $u_\lambda(x,0)$ and u_0 are the same (this is true for a Riemann initial data for instance), then (31) reduces to

$$E(T) = \frac{\displaystyle\int_{x_0}^{x_1} u_\lambda(x,T)dx - \int_{x_0}^{x_1} u(x,T)dx}{\displaystyle\int_{x_0}^{x_1} u_\lambda(x,T)dx},$$

in view of (30). In other words, $E(T)$ represents the relative conservation error of u at time T on interval $[x_0, x_1]$. On Figures 8 and 9, we show (for instance and without restriction) functions $T \to E(T)$ for the four test cases considered in previous section and associated with the choice $f(u) = u^3$ (tests A^1, B^1, C^1, D^1). We used $x_0 = -1$ and $x_0 = 4$, except for the third test case for which the computational domain was determinated by $x_0 = -4$ and $x_0 = 4$ (so that the mass of $u_\lambda(x,T)$ on interval $[x_0, x_1]$ does not become 0 for all T under consideration : $0 \leq T \leq 0.15$). For the first test case (Figure 8 - Left), no conservation error is made since our algorithm exactly reduces to the Roe scheme. In the second test case (Figure 8 - Right), we observe that the conservation error is decreasing in time towards 0. Recall that our algorithm and Glimm's random choice scheme are identical for this test case. Lastly, the last two simulations (Figure 9 - Left and Right), for which the

solutions contain classical as well as nonclassical waves, have very small (around 0.4% and 0.5%) conservation error although the mesh is pretty coarse (100 points by unit interval). To conclude this section, Figure 10 is concerned with the third test case when the *modified* algorithm proposed at the end of the previous section is used (see also Figure 6). We observe that the conservation error is still very small (around 0.3%), even a little bit less important than without modification in the two steps algorithm.

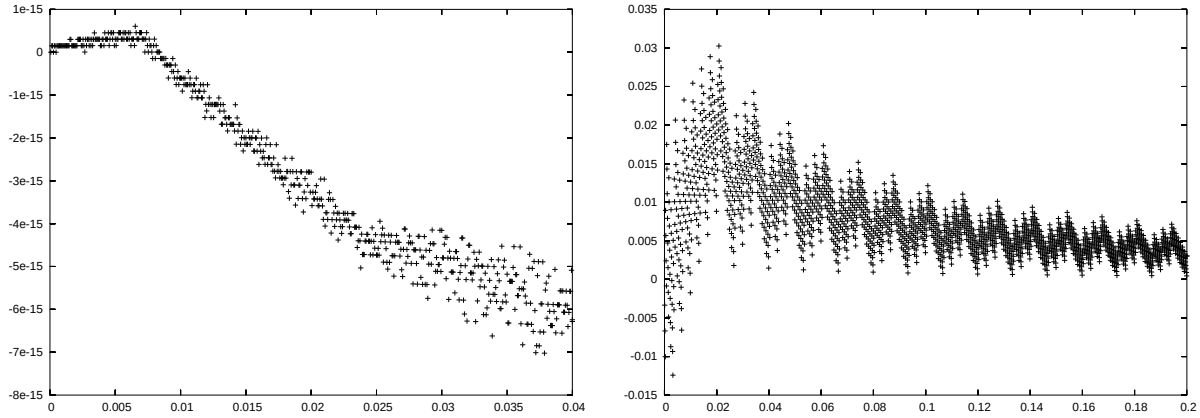

Figure 8: Conservation errors for classical solutions : test A^1 (Left) and B^1 (Right)

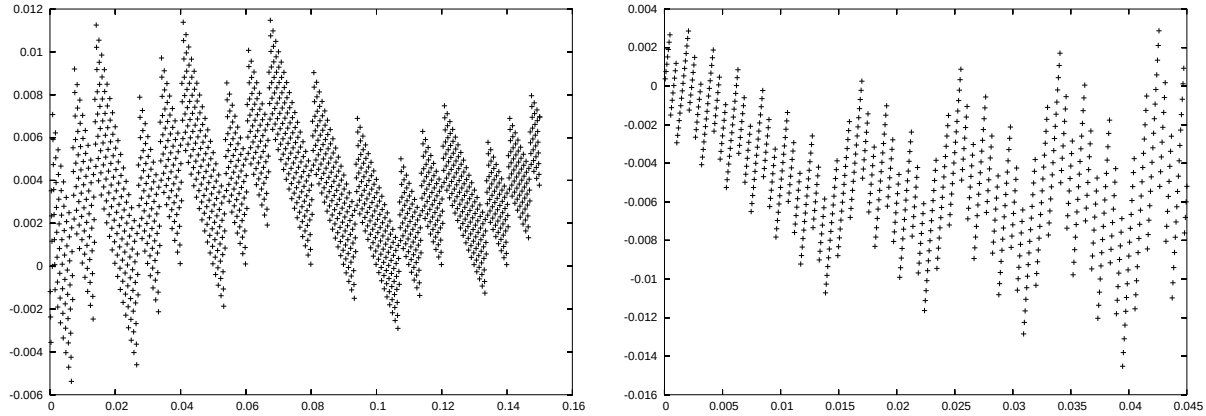

Figure 9: Conservation errors for nonclassical solutions : test C^1 (Left) and D^1 (Right)

7 Conclusion

We have presented a new powerful numerical strategy for approximating nonclassical solutions whose dynamics is dictated by a kinetic function. The main idea was the modification of a given conservative scheme in order to make properly captured the underlying undercompressive waves. We have seen that our algorithm reduces sometimes to Glimm's random choice scheme, and sometimes to the basic conservative scheme. Actually, our algorithm keeps advantages of Glimm's random choice scheme without its drawbacks since first, it does not depend on the knowledge of the (nonclassical) Riemann solution, and then it provides sharp interfaces propagating at the right

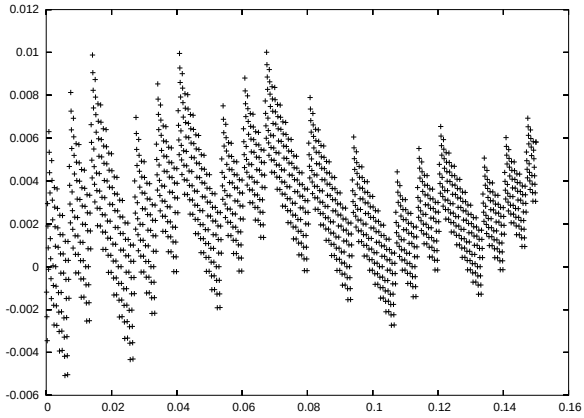

Figure 10: Conservation error for a nonclassical solution with the *modified* algorithm : test C^1

speed. A subsequent paper [5] is concerned with the stability properties of the scheme we have proposed together with its extension to the case of systems. In [4], we apply our numerical strategy to approximate the possibly nonclassical solutions of a macroscopic model for the description of the flow of pedestrians. This issue actually deserves a particular attention since the function playing naturally the role of a kinetic function $\varphi^\flat$ turns out to be neither invertible nor defined on the whole domain $\mathbb{R}$ in this context. Then, a suitable adaptation of the present algorithm is proposed.

References

[1] Abeyaratne R. et Knowles J.K., *Implications of viscosity and strain gradient effects for the kinetics of propagating phase boundaries*, SIAM J. Appl. Math., vol 51, pp 1205-1221 (1991).

[2] Amadori D., Baiti P., LeFloch P.G. and Piccoli B., *Nonclassical shocks and the Cauchy problem for non-convex conservation laws*, J. Differential Equations, vol 151, pp 345-372 (1999).

[3] Chalons C., *Bilans d'entropie discrets dans l'approximation numérique des chocs non classiques. Application aux équations de Navier-Stokes multi-pression 2D et à quelques systèmes visco-capillaires*, PhD Thesis, Ecole Polytechnique, (2002).

[4] Chalons C., *Numerical approximation of a macroscopic model of pedestrian flows*, Preprint of the Laboratoire Jacques-Louis Lions (2005).

[5] Chalons C., In preparation.

[6] Chalons C. and Coquel F., In preparation.

[7] Chalons C. et LeFloch P.G., *A fully discrete scheme for diffusive-dispersive conservation laws*, Numerisch Math., vol 89, pp 493-509 (2001).

[8] Chalons C. et LeFloch P.G., *High-order entropy conservative schemes and kinetic relations for van der Waals fluids*, J. Comput. Phys., vol 167, pp 1-23 (2001).

[9] Chalons C. et LeFloch P.G., *Computing undercompressive waves with the random choice scheme. Nonclassical shock waves*, Interfaces and Free Boundaries, vol 5, pp 129-158 (2003).

[10] Collela P., *Glimm's method for gas dynamics*, SIAM J. Sci. Stat. Comput., vol 3, pp 76-110 (1982).

[11] Hayes B.T. and LeFloch P.G., *Nonclassical shocks and kinetic relations : Scalar conservation laws*, Arch. Rational Mech. Anal., vol 139, pp 1-56 (1997).

[12] Hayes B.T. and LeFloch P.G., *Nonclassical shocks and kinetic relations : Finite difference schemes*, SIAM J. Numer. Anal., vol 35, pp 2169-2194 (1998).

[13] Hou T.Y., LeFloch P.G. and Rosakis P., *A Level-Set Approach to the Computation of Twinning and Phase Transition Dynamics*, J. Comput. Phys., vol 150, pp 302-331 (1999).

[14] Hou T.Y., LeFloch P.G. and Zhong X., *Converging Methods for the Computation of Propagating Solid-Solid Phase Boundaries*, J. Comput. Phys., vol 124, pp 192-216 (1996).

[15] LeFloch P.G., *Propagating phase boundaries: formulation of the problem and existence via the Glimm scheme*, Arch. Rational Mech. Anal., vol 123, pp 153-197 (1993).

[16] LeFloch P.G., **Hyperbolic Systems of Conservation Laws: The theory of classical and nonclassical shock waves**, E.T.H. Lecture Notes Series, Birkhäuser (2002).

[17] LeFloch P.G. and Rohde C., *High-order schemes, entropy inequalities, and nonclassical shocks*, SIAM J. Numer. Anal., vol 37, pp 2023-2060 (2000).

[18] LeFloch P.G. and Shearer M., *Nonclassical Riemann solvers with nucleation*, Proc. Royal Soc. Edinburgh, vol 134A, pp 941-964 (2004).